Ramjet Diffuser Flowfield Response to Large-Amplitude Combustor Pressure Oscillations

T. Hsieh* and A.B. Wardlaw Jr.*
Naval Surface Weapons Center, Silver Spring, Maryland
and
T. Coakley †
NASA Ames Research Center, Moffett Field, California

The unsteady flow of a two-dimensional ramjet diffuser is studied numerically by solving the Navier-Stokes equation with a two-equation turbulence model. Unsteadiness is introduced by prescribing a pressure disturbance at the diffuser exit plane. The case with a sinusoidal exit plane pressure flucutation of 20% of the mean exit pressure is considered to simulate pressure oscillation from a ramjet combustor. The resulting flowfield exhibits a complicated interaction between the terminal shock, separation pocket, and inviscid core flow. The exit plane flow properties feature a nonlinear response to the imposed sinusoidal pressure variation.

I. Introduction

RECENT tests of integral rocket/ramjet propulsion systems have exhibited undesirable, high-amplitude pressure fluctuations caused by combustion instabilities.[1] The most troublesome oscillations are in the frequency range of 100–500 Hz, and the corresponding root-mean-square pressure oscillation amplitudes can reach up to 20% of the mean combustor pressure. Figure 1 shows a schematic diagram of the main flow features expected from a typical ramjet engine under a direct-connect testing setup. The inlet is connected to the facility air supply through a plenum and the approaching flow is subsonic. Downstream of the inlet diffuser, liquid fuel is injected. The mixed air and fuel then enter the combustor and are ignited. The flowfield in the combustor contains the recirculation zone, the flame sheet, and a vortex-shedding shear layer. Following the recirculation zone, the turbulent boundary layer begins to develop. A nozzle at the end of the combustor exhausts the combustion products into the the ambient air. During this complicated process, featuring chemical and thermal reactions, instabilities can occur due to the coupling of the flow features described. Although a complete numerical simulation of the entire flowfield for the system is beyond reach, it is possible to treat components of the system separately. In this paper, the response of the inlet to a prescribed sinusoidal combustor pressure fluctuation imposed at the exit plane (see Fig. 2) of the diffuser is considered by numerically solving the Navier-Stokes equations. The resulting solution provides a description of the unsteady shock structure and separation pocket formation as well as exit plane flow properties. Conditions at the exit plane influence the combustor shear layer, which itself is thought to be a source of unsteadiness. Hence, exit plane flow properties are of particular interest.

Most existing analyses of the inlet are based on asymptotic solutions to inviscid or viscous models[2-4] or acoustic plus quasisteady shock methods.[5] In these treatments, the viscous effects are accounted for through an inviscid viscous approach or an effective configuration that simulates the boundary-layer displacement. The predictions of such models agree with experiments for special cases of small-amplitude oscillations in diffusers with little or no separation. In other situations, these approaches are questionable because they omit such relevant physical phenomena as shock wave and boundary interaction, flow separation, and reattachment. Successful applications of numerical procedures for solving the Navier-Stokes equations in unsteady diffusers have been reported in Refs. 6–8. However, these papers consider only low-amplitude fluctuations. In Ref. 9, the Navier-Stokes equations are applied to the study of diffusers featuring large-amplitude fluctuations and significant separation regions.

Extensive experimental investigations of unsteady diffuser flowfields have been reported by Sajben et al.,[10] Bogar et al.,[11] and Salmon et al.[12] Only small-amplitude pressure oscillations have been studied because of the practical difficulties associated in creating large, controlled pressure oscillation in the laboratory. On the other hand, it is relatively simple to prescribe a large-amplitude pressure oscillation in a numerical experiment. This paper describes such an experiment in which the Navier-Stokes equations are solved numerically for a two-dimensional, planar diffuser subject to a 20% amplitude and 300 Hz sinusoidal pressure fluctuation at the exit plane of the inlet. Special attention is directed toward the exit plane flow properties in order to understand better the coupling between the inlet and the combustor.

The numerical procedures are outlined in Sec. II, the results for unsteady calculations are given in Sec. III, and a summary is provided in Sec. IV.

II. Numerical Procedures

The numerical method used for solving the Navier-Stokes equations is described in Ref. 6. The time-dependent, mass-averaged, thin-layer Navier-Stokes equations for compressible flow are written in conservation form. A general coordinate transformation is used to map the physical plane into a rectangular computational grid. A modified version of MacCormack's hybrid method[13] is applied using the finite-volume approach. This method is second-order accurate in time and space. Total temperature and stagnation pressure are speci-

Presented as Paper 84-1363 at the AIAA/SAE/ASME 20th Joint Propulsion, Conference, Cincinnati, OH, June 11-13, 1984; received March 13, 1986; revision received Nov. 4, 1986.

*Aerospace Engineer, Associate Fellow AIAA.
†Research Scientist. Member AIAA.

fied at the inflow boundary, whereas static pressure alone is defined at the outflow plane boundary. Along the upper and lower walls of the inlet, no-slip boundary conditions are applied in conjunction with adiabatic wall conditions. These conditions are more fully discussed in Ref. 6. The k-ω^2 two-equation eddy viscosity model by Wilcox and Rubensin[14] is applied using the set of constants described in Ref. 8. The computer code has been verified in steady and small-amplitude forced oscillating flow calculations and reasonable agreement with experimental data[8,9] has been obtained. However, the accuracy of large-amplitude transient calculation has not been verified because of the lack of experimental data. Calculations for unsteady diffuser flow with self-excited oscillations successfully predict the underlying complex physical phenomena, thus lending credence to the present results.[16,17]

All calculations are carried out on a mesh with 80 points in the longitudinal direction and 50 points in the vertical direction. The mesh is exponentially stretched in the vertical direction near the upper and lower duct walls in a manner that assures the presence of at least two points in the laminar sublayer. To improve the resolution of the terminal shock, the longitudinal mesh points are clustered in the diffuser region, i.e., between $x/H=1$ and 3. Here, x is the axial distance along the diffuser, H the throat height, and $x=0$ occurs at the throat.

The initial flowfield is prescribed using the one-dimensional steady inviscid duct solution. Near the upper and lower walls, flow properties are modified using the one-seventh power law along with a linear laminar sublayer profile. Appropriate initial profiles for k and ω^2 are also implemented. Convergence to steady state is assumed when calculated properties do not vary significantly over 50 time steps. The unsteady boundary condition at the exit boundary is then imposed. Unsteady computations are carried out for a number of cycles until the flowfield is quasistationary. This required between 7 and 9 cycles or between 6300 and 8100 time steps.

The computational method proves to be very robust and, with little difficulty, provides solutions to a variety of exit boundary conditions, such as a large-amplitude pressure pulse, rapid increase of pressure, and sinusoidal pressure variation.[9] The calculations are performed on the NASA ARC Cray/XMP computer and use 3.6 (10^{-4}) CPU s/mesh point/time step.

III. Results and Discussion

The diffuser configuration considered in this paper is depicted in Fig. 2, and it has been experimentally investigated.[10-12] A detailed description of this diffuser is given in Ref. 10. For verification purposes, computations are carried out for the case of steady flow with R_p values of 0.72, 0.82, and 0.862, where R_p is defined as the pressure ratio of the exit plane pressure p_e to the reservoir pressure p_t. The calculations are set up with the inflow and outflow boundaries located at $x/H=-4$ and 8.6. As is shown in Fig. 2, the actual inlet extends from x/H of -6.93 to 14.43 and features three suction slots along the bottom and side walls of the inlet, which are not simulated in the calculations. For the cases considered in this paper, the reservoir pressure and temperature are 135 kPa and 526°R, respectively. This produces a Reynolds number at the inflow boundary, based on inflow inlet height, of 8.22×10^5.

The comparisons of steady flowfields between the calculations and the experiment are given in Ref. 9, and reasonable agreement is found despite the possible influence of three-dimensionality on the experimental results. As described in Ref. 9, the computation accurately predicts the length of the separation pocket but underpredicts its thickness. The computed zero velocity line lies about halfway between the wall and the measured zero velocity contour. Furthermore, on the downstream side of the separation pocket, the experiment indicates a fully developed channel flow, whereas the calculation features an inviscid core region. These differences are partially due to the three-dimensional effects in the experimental data as shown in the Mach contour plots on the exit cross section given in Ref. 10. Besides these differences, the numerical solution provides a correct qualitative prediction of the diffuser flowfield.

The numerical model is applied to the diffuser of Fig. 2 with a 300 Hz sinusoidal exit plane pressure fluctuation at the exit boundary. The amplitude of fluctuation is 20% of the mean static pressure, which is equal to $R_p=0.8$. The behavior of the top wall, bottom wall, and centerline pressures throughout a cycle is shown in Fig. 3, while the corresponding Mach number contours are given in Fig. 4. In Fig. 3, *Pd*, *Pu*, *R*, and *S* stand for pulse moving downstream, pulse moving upstream, reattachment point, and separation point, respectively. The pressure curves for the centerline and bottom wall coincide in Figs. 3a-3g and Figs. 3p-3r. In Fig. 4, B_t, B_s, and *TS* stand for bifurcation of wall pressure jump, bifurcation of separation pocket, and terminal shock, respectively; the dotted and broken lines represent the sonic and zero velocity lines, respectively. The time interval between each plot is 1/18th of a cycle or $\Delta\theta=\pi/9$ (20 deg), in which θ is the phase angle measured from the point in the cycle where the pressure is equal to its mean static value and $dp/dt>0$. In Figs. 3 and 4, the indicated separation and reattachment points are obtained from plots of the skin-friction distribution over the walls. More information can be found in Ref. 15 about instantaneous velocity profiles at six different axial stations and pressure contours at selected values of θ.

An examination of Figs. 3 and 4 suggests that the oscillation cycle can be divided into several distinct phases:

1) As illustrated in Figs. 3a-3d and Figs. 4a-4d, at the start of the cycle, the terminal shock appears ahead of the throat and moves upstream. The shock is weak and there is no flow separation throughout the diffuser. The shock becomes weaker as it moves upstream and finally turns into a pressure pulse (indicated by *Pu*) that propagates into the reservoir. Meanwhile, the increasing exit pressure raises pressure levels in the downstream section of the inlet.

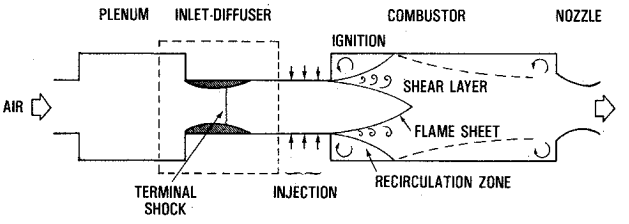

Fig. 1 Schematic diagram of a ramjet propulsion system.

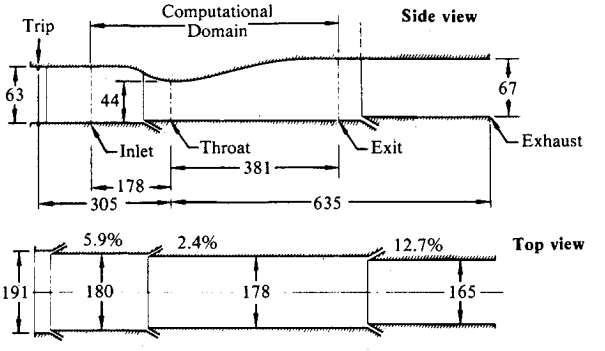

Dimensions in millimeters
Vertical dimensions doubled
Slot sizes enlarged for clarity
Percentages denote area decrease at slots

Fig. 2 Inlet-diffuser configuration (courtesy of M. Sajben).

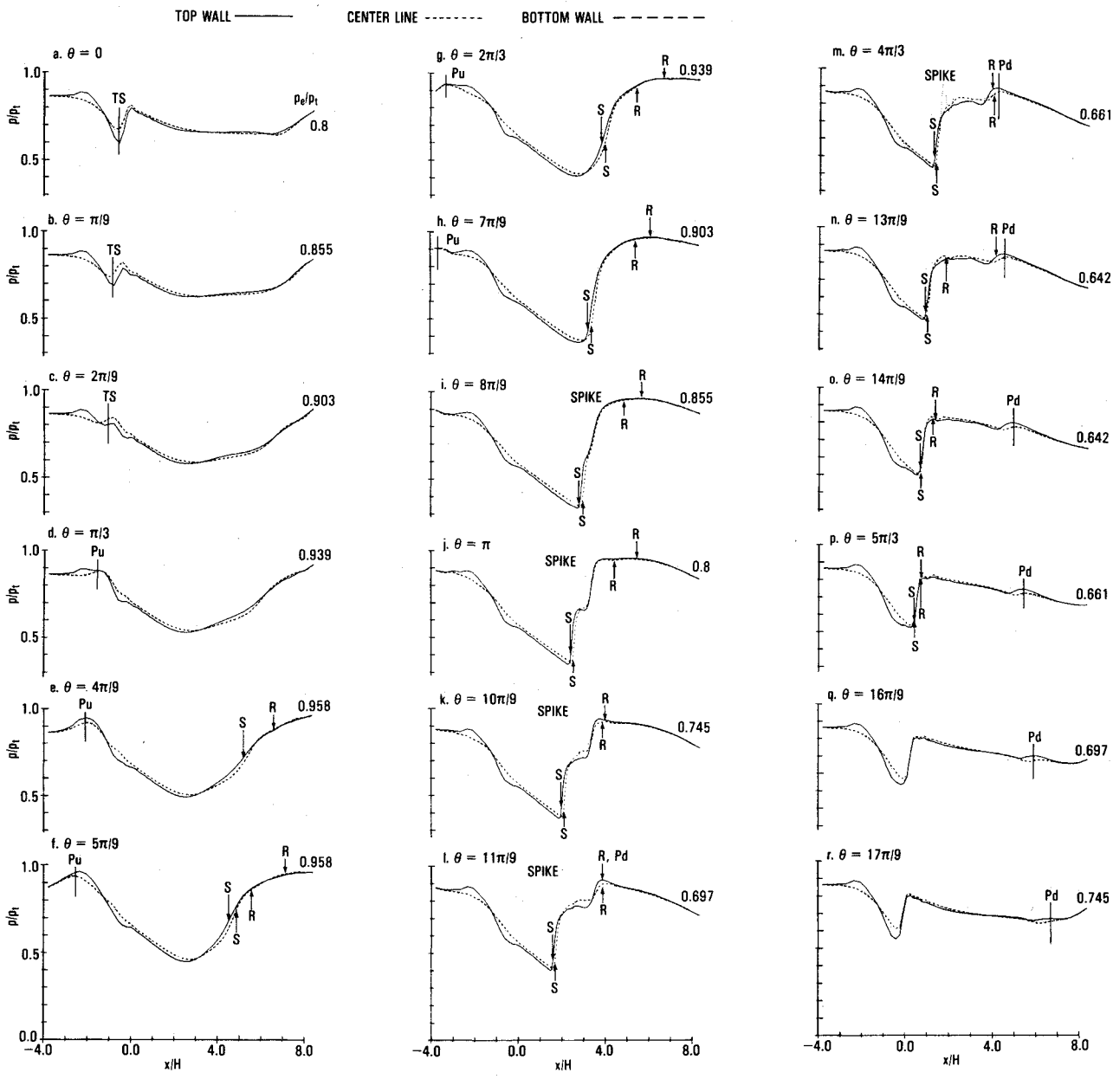

Fig. 3 Variation of inlet pressures to oscillatory exit pressure.

2) As illustrated in Figs. 3e–3h and Figs. 4e–4h, a sharp adverse pressure gradient gradually forms in the middle portion of the duct connecting the lower pressure levels near the throat with the higher levels in the downstream section of the duct. Flow separation, induced by the pressure gradient, appears first on the top and then later on the bottom wall. The separation points move upstream as the separation pockets on both walls grow. As time passes, the pressure gradient steepens into a curved shock that is much stronger near the centerline. The shock induces further flow separation on both walls, as shown by the thickening of the separation pocket immediately behind the shock (Fig. 4i).

3) As illustrated in Figs. 3i–3l and Figs. 4i–4l, along the inlet centerline, a pressure spike develops on the downstream side of the terminal shock, which is followed by a second region of adverse pressure gradient. Both the magnitude of the spike and the second adverse pressure gradient increase as the cycle progresses. Along the walls of the diffuser, the terminal shock-induced flow separation develops an intermediate pressure plateau. Here, the pressure spike is not visible. The pressure plateau covers the extent of the thickened portion of the separation pockets.

4) As illustrated in Figs. 3m–3r and Figs. 4m–4r, near the walls, the portion of the pressure rise downstream of the pressure plateau forms a downstream-moving pressure pulse as indicated by *Pd*. A similar pulse having a smaller amplitude forms near the diffuser centerline. The terminal shock moves forward to the position it occupied at the start of the cycle and separation pockets disappear. On the top wall, separation first bifurcates and then disappears.

Exit plane conditions provide the coupling between the inlet and combustor portion of a ramjet. From the point of view of understanding the dynamic characteristics of the entire system, it is necessary to focus attention on the exit plane flowfield variations. Both acoustic theory and small-perturbation models[9] predict that the sinusoidal pressure variations at the exit plane will generate sinusoidal velocity variation of the same frequency, but with altered phase angle and amplitude. By contrast, the Navier-Stokes solution obtained in this study features a nonsinusoidal exit plane velocity variation in response to an imposed sinusoidal pressure fluctuation. This is illustrated in Fig. 5 where the variation of $\Delta U = U - \bar{U}$ over a cycle is shown at the exit plane at various heights Y/Y_m. Here, U and $\bar{U}$ are the instantaneous and mean

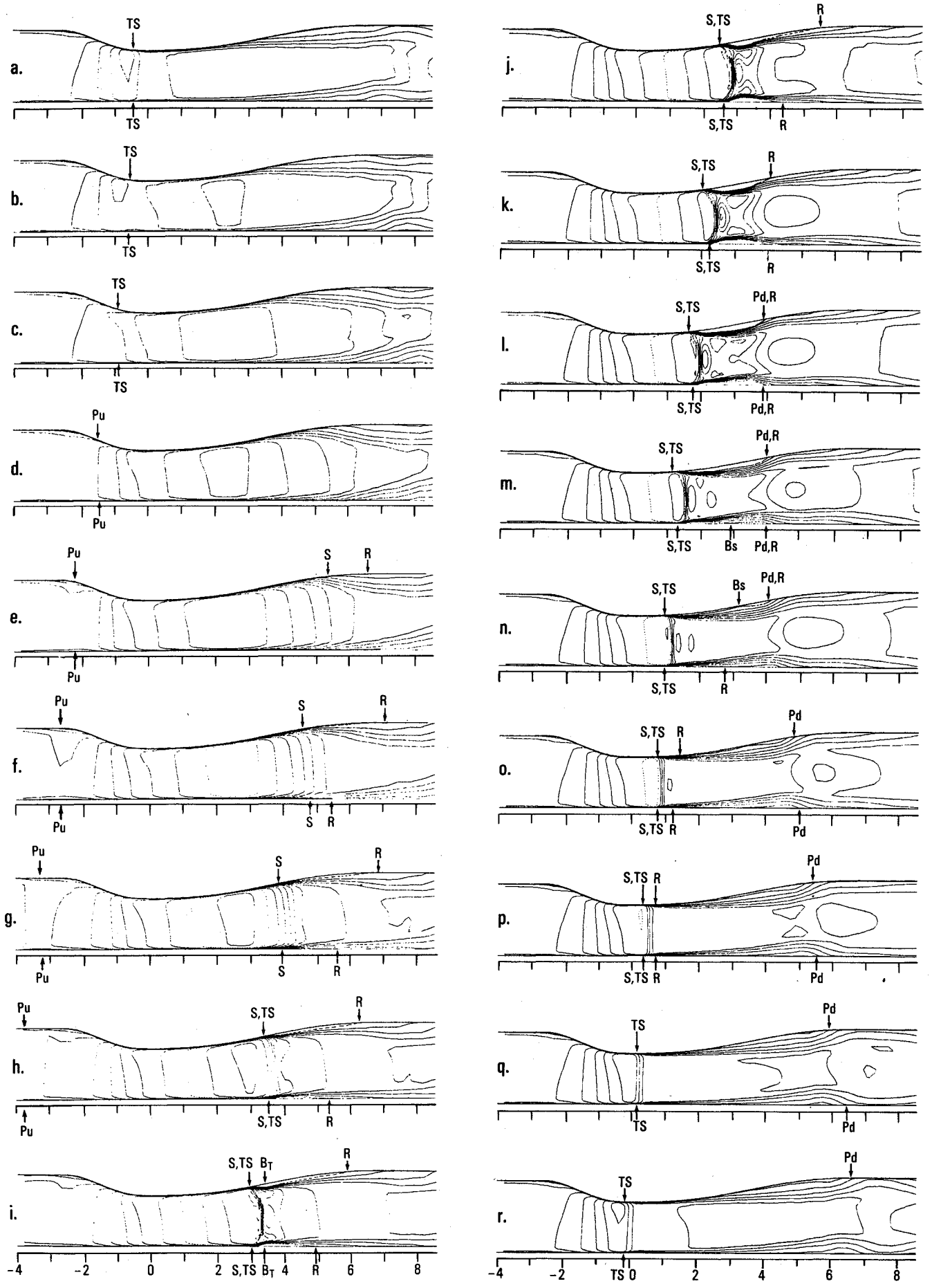

Fig. 4 Mach contour response to oscillatory exit pressure.

streamwise exit velocities, respectively, Y the vertical distance from the bottom wall, and Y_m the vertical distance between the top and bottoms walls. The variation of the pressure recovery factor α, which is the ratio of the sum of static and dynamic pressure at the exit plane to the reservoir pressure, is shown throughout a cycle in Fig. 6; the top and bottom wall displacement thicknesses δ_t and δ_b, respectively, are given in Fig. 7. Here displacement thickness is defined as

$$\delta = \frac{1}{U_m}\int_0^{\delta_m}(U_m - u)\,dy$$

where U_m and u are the instantaneous maximum and the local streamwise velocities in the boundary layer, respectively, and δ_m is the distance from the wall at which the maximum velocity occurs. Lack of a clear boundary between the boundary layer and the inviscid core necessitates the use of these displacement thickness definitions. Velocity profiles at the exit plane (nondimensionalized by the core velocity at the throat, $U^* = 310$ m/s) are shown at a number of different phase angles in Fig. 8. An examination of Figs. 5-8 indicates that, during the first half of the cycle when the exit pressure is greater than the average pressure, the velocity at the exit plane is at a minimum and the recovery pressure and the displacement thicknesses are at a maximum. During this period, the flow throughout the diffuser is primarily subsonic and strong shocks are not evident. During the second half of the cycle, when the exit pressure is less than the average pressure, strong shocks and large separation pockets appear and the exit plane

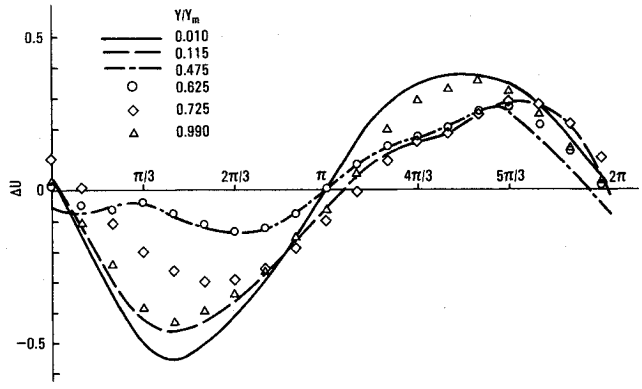

Fig. 5 Variation of exit plane Δu at different heights over a cycle.

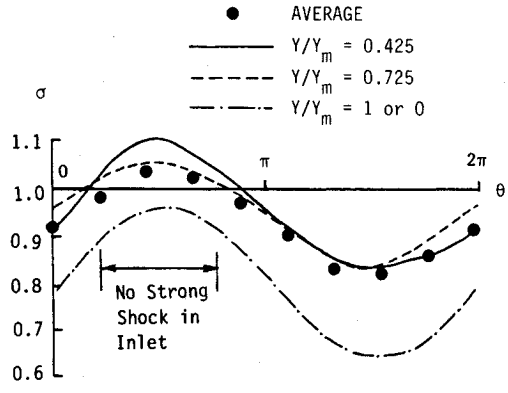

Fig.6 Variation of exit plane pressure recovery at different heights over a cycle.

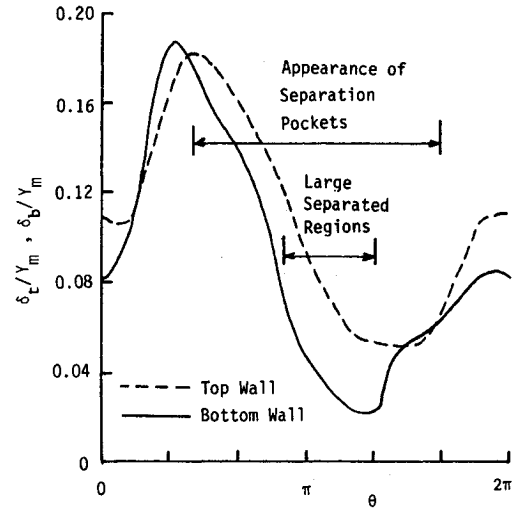

Fig. 7 Variation of exit plane boundary-layer thickness over a cycle.

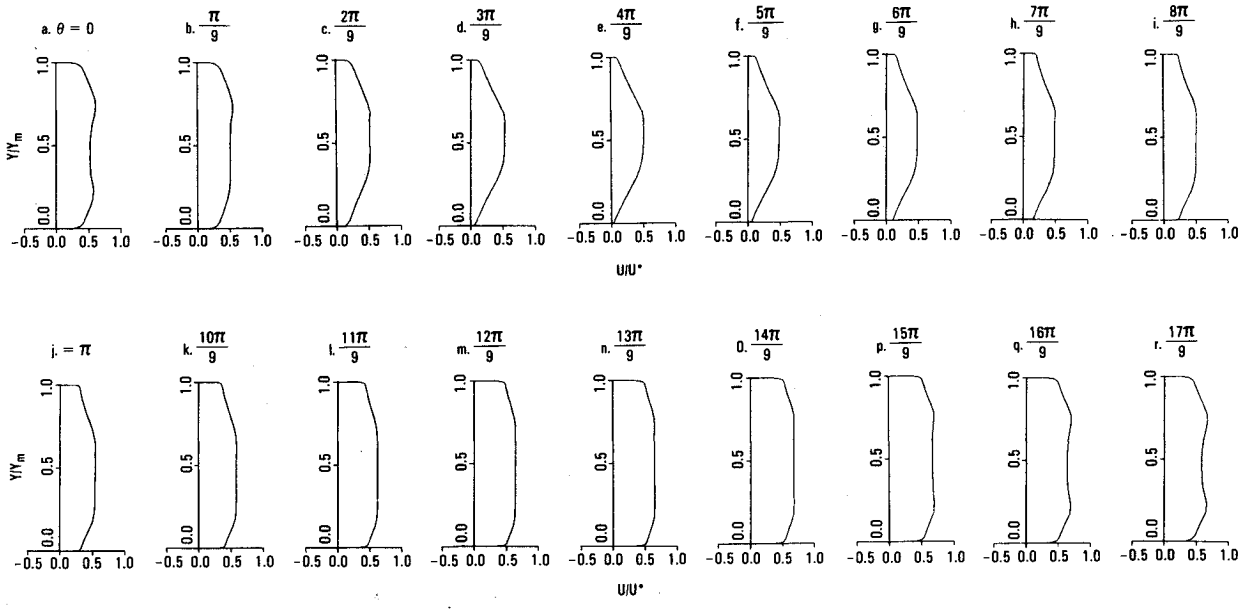

Fig. 8 Variation of exit plane axial velocity profile over a cycle.

velocity reaches a maximum, while the recovery pressure and displacement thicknesses achieve minimum values.

IV. Conclusions

Unsteady flow calculations were performed for a two-dimensional ramjet diffuser by solving Navier-Stokes equations with a two-equation turbulence model. A 300 Hz sinusoidal pressure disturbance with an amplitude of 20% of the mean static pressure was applied to the exit plane. The resulting flowfields suggest that viscous effects play a dominant role. The strong interactions among the terminal shock, the separation pocket, and the inviscid core flow contain a number of notable features:

1) Curved terminal shocks that disappear and reform as the unsteadiness progresses.

2) Division of the terminal shock into two branches, a main one that moves upstream into the throat and a second that is swept downstream toward the exit plane.

3) Separation region formation, bifurcation, and disappearance. In addition, examination of the exit plane properties indicates that a sinusoidal, large-amplitude pressure fluctuation generates nonsinusoidal variations in exit plane velocity and recovery pressure. Large variations in the exit plane velocity profile and boundary-layer thickness over a cycle will probably have a great influence on the combustor flowfields. The computed flowfields appear to be plausible; however, the accuracy of the calculation remains to be determined since experimental data are not available for comparison.

Acknowledgments

This work was partly sponsored by the Naval Weapons Center and the Office of Naval Research and monitored by Drs. W.C. Clark and R.E. Whitehead. The computer time for the calculation was provided by NASA Ames Research Center, Applied Computational Aerodynamics Branch. Eva Pegot of NASA's Experimental Fluid Dynamics Branch assisted with the computer plots.

References

[1]Clark, W.J., "Experimental Investigation of Pressure Oscillations in a Solid Dump Ramjet Combustor," *Journal of Spacecraft and Rockets,* Vol. 19, Jan.-Feb. 1982, pp. 47-53.

[2]Richey, G.K. and Adamson, T.C. Jr., "Analysis of Unsteady Transonic Channel Flow with Shock Waves," *AIAA Journal,* Vol. 14, Aug. 1976, pp. 1054-1061.

[3]Adamson, T.C. Jr., Messiter, A.F., and Liou, M.-S., "Large Amplitude Shock Wave Motion in Two-Dimensional Transonic Channel Flows," *AIAA Journal,* Vol.16, Dec. 1978, pp. 1240-1247.

[4]Liou, M.-S. and Sajben, M., "Analysis of Unsteady Viscous Transonic Flow with a Shock Wave in a Two-Dimensional Channel," AIAA Paper 80-0195, 1980.

[5]Culick, F.E.C. and Rogers, T., "Modeling of Pressure Oscillations in Ramjets," AIAA Paper 80-1192, 1980.

[6]Coakley, T.J. and Bergmann, M.Y., "Effects of Turbulence Model Selection on the Prediction of Complex Aerodynamic Flow," AIAA Paper 79-0070, 1979.

[7]Liou, M.-S., Coakley, T.J., and Bergmann, M.Y., "Numerical Simulation of Transonic Flows in Diffuser," AIAA Paper 81-1240, 1981.

[8]Liou, M.-S. and Coakley, T.J., "Numerical Simulations of Unsteady Transonic Flow in Diffuser," *AIAA Journal,* Vol. 22, Aug. 1984, pp. 1139-1145.

[9]Hsieh, T., Wardlaw, A.B. Jr., Collins, J.P., and Coakley, T.J., "Numerical Investigation of Unsteady Inlet Flow Field," *AIAA Journal,* Vol. 25, Jan. 1987, pp. 75-81.

[10]Sajben, M., Bogar, T.J., and Kroutil, J.C., "Forced Oscillation Experiments in Supercritical Diffuser Flows with Applications to Ramjet Instabilities," AIAA Paper 81-1487, 1981.

[11]Bogar, T.J., Sajben, M., and Kroutil, J.C., "Characteristic Frequencies of Transonic Diffuser Flow Oscillations, *"AIAA Journal,* Vol. 21, Sept 1983, pp. 1232-1240.

[12]Salmon, J.T., Bogar, T.J., and Sajben, M., "Laser Velocimeter Measurements in Unsteady, Separated, Transonic Diffuser Flows," AIAA Paper 81-1198, 1981.

[13]MacCormack, R.W., "An Efficient Numerical Method for Solving the Time-Dependent Compressible Navier-Stokes Equations at High Reynolds Number," *Computing in Applied Mechanics,* Vol. 18, Dec. 1976, pp. 49-64.

[14]Wilcox, D.C. and Rubesin, M.W., "Progress in Turbulence Modeling for Complex Flowfield Including Effects of Compressibility," NASA TP 1517, 1980.

[15]Hsieh, T., Wardlaw, A.B., and Coakley, T.J., "Numerical Simulation of a Ramjet Inlet Flowfield in Response to Large Amplitude Combustor Pressure Oscillation," AIAA Paper 84-1363, 1984.

[16]Hsieh, T., Bogar, T.J., and Coakley, T.J., "Numerical Simulation and Comparison with Experiment for Self-Excited Oscillations in a Diffuser Flow," *AIAA Journal,* Vol. 25, July 1987, pp. 936-943.

[17]Hsieh, T. and Coakley, T.J., "Unsteady Separated Boundary Layer in a Transonic Diffuser Flow with Self-Excited Oscillations," AIAA Paper 86-1037, May 1986.